J. Biochem. 128, 923–932 (2000)

Identification of a Novel WD Repeat–Containing Gene Predominantly Expressed in Developing and Regenerating Neurons

Hiroaki Kato,* Shi Chen,* Hiroshi Kiyama,† Ken Ikeda,‡ Naoki Kimura,* Kinichi Nakashima,*,§ and Tetsuya Taga*,§,[1]

*Department of Molecular Cell Biology, Medical Research Institute, Tokyo Medical and Dental University, 2-3-10, Kanda-surugadai, Chiyoda-ku, Tokyo 101-0062; †Department of Anatomy, Asahikawa Medical College, 4-5-3-11, Nishikagura, Asahikawa 078-8510; ‡Fourth Department of Internal Medicine, 2-17-6, Ohashi, Meguro-ku, Tokyo 153-0044; and §Department of Cell Fate Modulation, Institute of Molecular Embryology and Genetics, Kumamoto University, 2-2-1, Honjo, Kumamoto 860-0811

Received July 24, 2000; accepted September 19, 2000

In the present study, we have identified a novel gene, NDRP (for neuronal differentiation-related protein), which is predominantly expressed in developing and regenerating neurons. The predicted NDRP comprises 1,019 amino acid residues and has 6 WD repeats in the N-terminal half and multiple potential nuclear localization signals (NLSs) at the C-terminal part. This molecule shows no significant structural similarity with any other molecules in available databases. *In situ* hybridization and immunohistochemistry revealed the highest expression of NRDP in sensory neurons, for instance, olfactory epithelia and neural layer of retina during embryonic development, as well as in perinatal dorsal root ganglions. The expression of this gene in intact motor neurons such as in the hypoglossal nerve was undetectable but became obvious after axotomy. These results suggest that the product of this gene might be involved in the development of sensory neurons as well as the regeneration of motor neurons.

Key words: motor neuron, nerve regeneration, neural development, sensory neuron, WD repeats.

The mechanisms regulating neuronal development and maintenance during development, and regeneration upon injury may involve a variety of genes. A useful approach to understand such mechanisms is to identify and characterize genes whose expression is restricted to a defined class of neurons or to a pathological condition. In an attempt to identify new genes from this viewpoint, we have tried to isolate genes whose expression is upregulated or downregulated in Wobbler mouse, a model of inherited motor neuron disease. We here report the isolation of a new gene encoding WD repeat–containing protein, NDRP (for neuronal differentiation–related protein), which has no significant similarity with any known molecules except WD motifs. We will discuss the functional property of this molecule based on our findings that NDRP (i) has multiple nuclear localization signals, (ii) shows predominant expression in neurons in retina and olfactory epithelia during embryonic development, (iii) exhibits upregulated expression in hypoglossal motor neurons after injury, and also based on the previous notion that WD repeat-containing proteins are generally regulatory proteins and versatile for diverse functions such as signal transduction (*1*), RNA processing (*2*), gene regulation (*3*, *4*), vesicular traffic (*5*), and regulation of cytoskeletal assembly (*6*) and/or cell cycle (*7*).

[1] To whom correspondence should be addressed. Tel/Fax: +81-96-373-6610, E-mail: taga@kaiju.medic.kumamoto-u.ac.jp

Abbreviations: DRG, dorsal root ganglion; ELISA, enzyme-linked immunosorbent assay; GCL, ganglion cell layer; GFAP, glial fibrillary acidic protein; GST, glutathione S-transferase; IGL, inner granular layer; IPL, inner plexiform layer; NDRP, neuronal differentiation–related protein; MAP2, microtubule-associated protein 2; OGL, outer granular layer; OMP, olfactory marker protein; OPL, outer plexiform layer; NLS, nuclear localization signal; NVL, neuroblastic ventricular layer; PB, phosphate buffer; PL, pigment layer; UTR, untranslated sequence.

EXPERIMENTAL PROCEDURES

Subtractive PCR Cloning of NDRP—NDRP cDNA was isolated from Wobbler mouse, which is an experimental animal model of motor neuron disease relevant to amyotrophic lateral sclerosis and spinal muscular atrophy (*8*, *9*). Total RNA prepared from the cervical spinal cord of Wobbler mouse when the animals began to display forelimb weakness and paralysis, was subjected to cDNA synthesis and PCR amplification by using a SMART PCR cDNA Synthesis Kit (Clonetech) according to the user's manual. Subtractive PCR cloning was performed by using a PCR-Select cDNA Subtraction Kit (Clonetech). Briefly, total RNA (one microgram) from Wobbler or control mouse was reverse-transcribed, and amplified by long distance PCR for 22 cycles with PCR primer and Advantage Klen Taq Polymerase. Double-strand cDNA was purified by chromatography with CHROMA SPIN-1000 (Clonetech) and used for *Rsa*I digestion. The subtraction was performed with a "tester" cDNA from Wobbler mouse and a "driver" cDNA from control mouse. By screening of 200 clones of the library with the subtracted tester cDNA and unsubtracted driver cDNA, 8 positive clones were obtained. A 1,038-bp fragment of NDRP cDNA was one of the clones obtained by these procedures. This fragment (558–1595 of NDRP cDNA

in Fig. 1A) was used to screen a randomly hexamer- and oligo-dT–primed λgt10 cDNA library from Swiss Webster/NIH embryo (Mouse 17-day Embryo 5′-STRECH PLUS cDNA, Clonetech). The inserts of positive clones were sequenced with a Dye Terminator Cycle Sequencing Ready Reaction Kit and ABI PRIZM 377 DNA Sequencer (PE Applied Biosystem), yielding a novel clone defining a 3,317-bp sequence.

Preparation of In Situ Probes—In situ probes for NDRP were constructed from 15.5 dpc mouse embryo by RT-PCR. Gel-purified XhoI/XbaI fragments (Probe 1, 33–548 nt; Probe 2, 1561–2184 nt) of NDRP were directionally subcloned into pSp73 (Promega). The region encompassing the WD repeats was not included in these probes to minimize cross-hybridization to other WD repeat–containing genes. ^{35}S-UTP–labeled antisense and sense probes were generated by using Riboprobe *in vitro* Transcription System (Promega) according to the technical manual.

Axotomy of Rat Hypoglossal Nerve—Male Wistar rats weighing approximately 100 g were anesthetized with pentobarbital (45 mg/kg) and positioned supine. Their right hypoglossal nerve was exposed and sectioned just proximal to its bifurcation at the level of the hyoid bone. Animals were decapitated under ether anesthesia on post-operative days 1, 3, 7, 14, and 21. Their brains were rapidly removed, frozen in powdered dry ice and stored at –80°C until sectioning. In this study, rats as well as mice were treated according to the guidelines of Tokyo Medical and Dental University.

Preparation of Tissue Sections—Adult mouse brains (ICR, 8 weeks old) and whole embryos (at various stages) were frozen in powdered dry ice or embedded with cryomatrix (Tissue-Tek O.C.T. Compound) and frozen in isopropyl alcohol (–80°C). Coronal and sagittal sections of 10 μm thickness were prepared with a cryostat (LEICA CM1900), thaw-mounted on (3-aminopropyltriethoxy)silane-coated microslide glasses, air-dried and stored at –80°C until *in situ* hybridization analysis. For immunohistochemistry 6-μm sections were prepared.

In Situ Hybridization—In situ hybridization was performed essentially as described by Kiryu *et al.* (*10*). Sections prepared above were fixed in 4% (w/v) paraformaldehyde/0.1 M phosphate buffer (PB) for 20 min at room temperature, washed twice with 0.1 M PB (5 min each). The brain sections were further treated with 10 μg/ml of proteinase K for 5 min, washed with 0.1 M PB, and fixed in 4% (w/v) paraformaldehyde/0.1 M PB for 5 min at room temperature. The embryo and brain sections were then placed in freshly mixed 0.25% acetic anhydride in 0.1 M triethanolamine for 10 min at room temperature, washed with 0.1 M PB, dehydrated serially with 70, 95, and 100% ethanol each for 2 min, treated with chloroform for 10 min, and washed with 100 and 95% ethanol for 2 min. ^{35}S-UTP labeled cRNAs (5×10^6 cpm/ml) of either antisense or sense probes were added to hybridization buffer (50% formamide, 10% dextran sulfate, 1× Denhardt solution, 200 μg/ml salmon sperm DNA, 0.2% sodium *N*-lauroylsarcosine, 500 μg/ml yeast t-RNA, 20 mM Tris-HCl pH 8.0, 5 mM EDTA, 10 mM PBS, 0.3 M NaCl, 2 mM DTT) and heated for 5 min at 100°C. The hybridization was performed with cover glasses overnight at 55°C in a humidified chamber. Slides were placed vertically in slide racks and immersed in a container of 5× SSC, 1% β-mercaptoethanol at 55°C until the cover glasses were released from the slides. The slides were washed in 50% formamide, 2× SSC, 10% β-mercaptoethanol at 65°C for 30 min (high stringency wash). After washing the slides 3 times with 10 mM Tris-HCl pH 7.5, 1 mM EDTA, 0.5 M NaCl (RNase buffer) for 10 min, the sections were treated with 1 μg/ml RNase A in RNase buffer for 30 min at 37°C. The slides were then washed at 37°C with RNase buffer for 10 min, followed by serial washes with high stringency wash (65°C, 30 min), 2× SSC (room temperature, 10 min), 0.1× SSC (room temperature, 10 min). The sections were dehydrated with 70, 95, and 100% ethanol, dried at room temperature, then exposed to films (X-OMAT AR, Eastman Kodak) for 4 days to determine the exposure period required for emulsion autoradiography. The slides were dipped in Kodak NTB-2 emulsion (Eastman Kodak) diluted 2:3 with distilled water, air-dried, stored in a light-tight box and exposed at 4°C for 2–3 weeks. They were developed with Kodak D-19, fixed with Fuji-Fix (Fuji-Film), counterstained with cresyl violet, dehydrated in a graded series of ethanol to xylen, and coverslipped for observation, which was performed under a light microscope with dark-filed condensers.

Generation of Antibody against NDRP—Rabbits were immunized with NDRP fused to glutathione S-transferase (GST-NDRP fusion protein translated in *E. coli* BL-21 from pGEX4T-3/NDRP constructs; amino acid residues between 696 to 863). Two hundred micrograms of the fusion protein was mixed with 800 μg of *N*-acetyl-*d*-glucosaminyl-(β1-4)-acetyl-*l*-alanyl-*d*-isoglutamin (GMDP) (*11*) in 1 ml of phosphate-buffered saline (PBS; 10 mM PB, 0.137 M NaCl, 2.7 mM KCl, pH 7.4) and emulsified with 1 ml of incomplete Freund's adjuvant. After four subcutaneous injections at intervals of 10 days, antiserum was preadsorbed onto a GST-coupled Sepharose 4B column, then purified with Sepharose 4B immobilized with GST-NDRP fusion protein. Anti-NDRP immunoreactivity of purified antiserum and removal of anti-GST antibody from purified antiserum were confirmed by ELISA, using GST and GST-NDRP as coating antigen.

Immunohistochemistry—Sections rinsed in PBS to wash out the cryomatrix were fixed in 4% (w/v) paraformaldehyde/PBS for 20 min at room temperature and washed twice with PBS (5 min each). Nonspecific binding was blocked by incubating the sections for 1 h at room temperature in PBS/0.1% Triton X-100 containing 1% bovine serum albumin (blocking buffer). Sections were then incubated overnight at 4°C with affinity-purified anti-NDRP (3 μg/ml in blocking buffer). After three washes in PBS (10 min each), sections were reacted with rhodamine-conjugated donkey anti-rabbit immunoglobulin (IgG; Chemicon; diluted 1:300 in 5% normal donkey serum/PBS) at room temperature for 30 min. After three washes in PBS (10 min each), sections were incubated for nuclear staining in PBS containing Hoechst 33258 (1 μg/ml) for 15 min.

The specificity of NDRP labeling was tested in various control conditions including (a) omission of anti-NDRP antibody from the staining procedures, (b) substitution of anti-NDRP antibody with normal mouse IgG at a 3-fold higher concentration (9 μg/ml), and (c) use of anti-NDRP antibody preparation adsorbed with 100-fold excess (weight ratio) of GST-NDRP fusion protein.

RESULTS

Structural Feature of NDRP—A full-length NDRP was cloned from λgt10 mouse embryo cDNA library and found to contain an open reading frame of 3,057 nucleotides (encoding 1,019 amino acid residues) which is flanked by a 117-nt long 5′ untranslated sequence (UTR) and a 140-nt long 3′ UTR (Fig. 1A). The 3′ untranslated sequence does not contain a polyadenylation signal, indicating the existence of more 3′UTR at a C-terminal site.

A search for proteins homologous with the isolated clone in the DNA Data Bank of Japan revealed the presence of six short sequences known as WD-repeats (or Gβ-repeats) at positions 181–211, 223–253, 265–299, 353–393, 417–452, and 464–495 (Fig. 1A, bold-faced and underlined; Fig. 1B, numbered from 1 to 6). One WD-unit perfectly matches the consensus (unit 6), and the other five contain one (in units 1 and 2) or two (in units 3–5) mismatches (Fig. 1C). This result fits the criteria that proteins in the WD-repeat family should contain at least one unit that matches the expression with no or one mismatch, and one or more additional units that have fewer than three mismatches (*12*). NDRP thus qualifies as a member of the WD-repeat family. One WD unit (core-region) is characterized by 27 ± 2 amino acids (aa), usually beginning with glycine-histidine (GH) and ending with tryptophane-aspartic acid (WD) (*12*, *13*). In NDRP protein, the number of aa in each unit was relatively constant in units 1, 2, and 6 (31–32), but was greater in units 3 to 5 (35–41). As shown schematically in Fig. 1B, the lengths of the spacers between units (WD to downstream GH, also called non-core regions) are constant (11 aa) in the first, second and fifth gaps, consistent with the regular length of 11 ± 2 (*12*, *13*), while those in the third and fourth spaces are longer and of variable length (23–53 aa). The amino acid sequences of these five spacers also have no similarity to any sub-family of the WD repeat–containing protein, implying novel function in this protein. By searching for protein sorting signals, we found potential nuclear localization signals (NLSs) in the carboxyl terminal part of NDRP. There are two 4-residue patterns (called "pat4") composed of 4 basic amino acids (K or R), at positions 756 and 913, in the amino acid sequence of NDRP (Fig. 1A, underlined; Fig. 1B, dark rectangles). The other (called "pat7") is a pattern starting with P followed within 3 residues by a basic segment containing 3 K/R residues out of 4 (*14*). Pat7 is present at positions 870, 909, 912, and 917. Another type of NLS (called "bipartite") is composed of 2 basic residues, a 10-residue spacer, and another basic region comprising at least 3 basic residues out of 5 residues (*15*). A probable bipartite-type NLS is present at positions 900–916. The region between 900 and 923 contains overlapping NLSs in the above three categories (pat4, pat7, and bipartite). The presence of multiple NLS suggests that NDRP may be a nuclear protein.

Strong Expression of NDRP in Olfactory Epithelia and Retina of Mouse Embryo—NDRP mRNA expression in mice during prenatal development was examined by *in situ* hybridization. In this experiments, we used two cRNA probes for different parts of NDRP (probes 1 and 2 in Fig. 1B), which gave essentially the same results. The respective sense probes gave no hybridization signal. No signals were seen when tissue sections were pretreated with 10 μg/ml RNase A before hybridization.

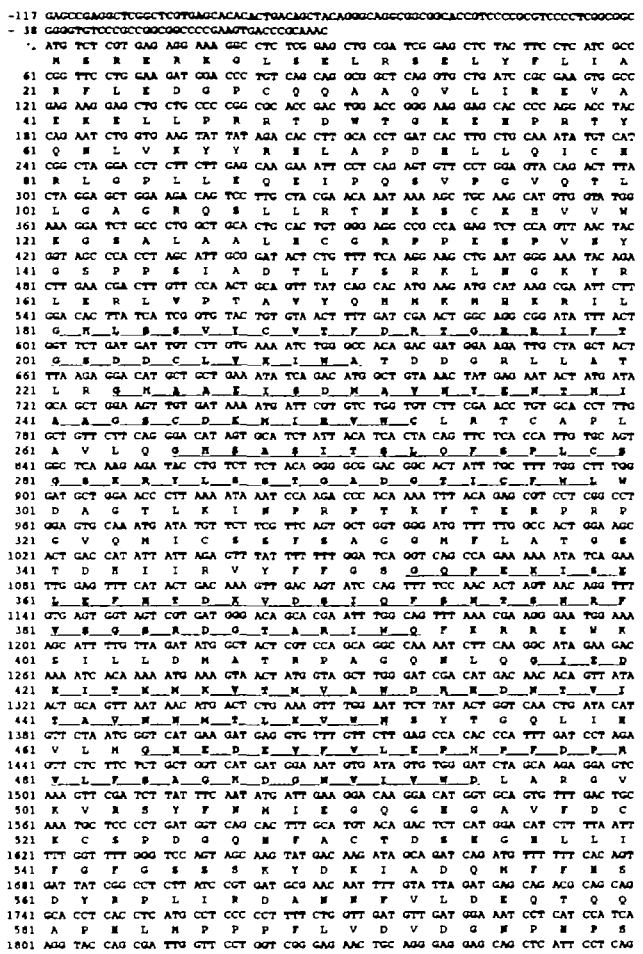

Fig. 1A

In mouse embryo, signals were not significantly detect-

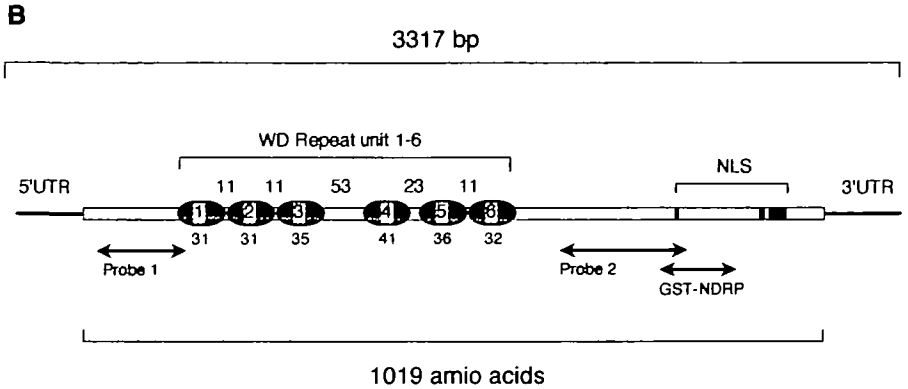

C

WD-Rpeats consensus regular expression																	Miss match
	W A S GH	XXX	A C M F V I LXXL	{1,7} X	W Y F V I {0,3} L X	{0,2} D D G G N N PXXP	{2 of 3} A C M F V {0,4} I X L SSS GGG X	D N	A C M F V I XXLX	A C M F K V YR I FN L WD	
Unit 1	GH	LSS	VYCV	T.....	F ...	DRTG	R RIF TGS D	D	CLVK	I WA	1
Unit 2	GH	AAE	ISDM	A.....	V ...	NYEN	T MIA AGS C	D	KMIR	V WC	1
Unit 3	GH	SAS	ITSL	QFSP...	L CS	GSK.	R YLS STG A	D	GTIC	F WL	2
Unit 4	GQ	PEK	ISEL	EFHTDKVDS	I QFS	NTSN	· RFV SGS R	D	GTAR	I WQ	2
Unit 5	GI	EDK	ITKM	KVTMVA.	W ...	DRHD	N TVI TAV N	N	MTLK	V WN	2
Unit 6	GH	EDE	VFVL	EPHP...	F ...	D..P	R VLF SAG H	D	GNVI	V WD	0

Fig. 1. **(A) Nucleotide and predicted amino acid sequences of NDRP cDNA.** Nucleotides are numbered from the first base of the putative initiation codon. The amino acid sequence, in single-letter code, is shown below the nucleotide sequence. The sequences of six WD repeats are bold-faced and underlined. Three clusters of putative nuclear localization signals are under-lined. **(B) Schematic representation of NDRP structure.** The single straight line depicts the 5′ and 3′ UTR regions of the cDNA; protein coding sequence is shown as a box. Six ovals correspond to the WD repeats, numbered 1–6. The lengths (*i.e.* the numbers of amino acid residues) of each WD repeat and each space between the WD repeats are indicated below and above the figure, respectively. Three clusters of NLS are also indicated. The probe for *in situ* hybridization and a fragment for GST-fusion are shown below the figure. **(C) Alignment of conserved core regions of the WD repeats in NDRP.** The WD repeat consensus is shown in the upper part of the figure. Well conserved motifs are boxed. Any amino acid in a vertical column may appear at that position. X means any amino acid. The number in curly brackets above the symbols represents variations in the number of amino acid residues. The number of mismatches in each WD repeat is shown to the right.

able until 12.5 dpc, when very weak signals were distributed throughout the embryo (data not shown). On 17.5 dpc, hybridization signals became clearer, and the highest NDRP transcripts were observed in the neural layer of the retina and olfactory epithelia, while moderate hybridization signals were detected in the dorsal part of the spinal cord and trigeminal ganglion (Fig. 2B). Strong hybridization signals were also detected in the striatum and neopallial cortex (Fig. 2D). In addition, moderate signals also became detectable in the mantle layer of the medulla oblongata, pons, diencephalon, midbrain, cerebellar primordium, spinal cord, and primordia of upper and lower incisor teeth on 17.5 dpc (Fig. 2D). As it is known that the precursors of neurons are present in the mesenchyme of developing tooth, which originate from the cranial neural crest (*16, 17*), NDRP appears to be widely expressed in neural tissues. Besides neural tissues, mRNA was detected in thymus, lung, and submandibular gland on 17.5 dpc (Fig. 2D). However, signals in these non-neural tissues decreased with development and were not detected in adult mouse (data not shown). The results from *in situ* hybridization analysis of prenatal mice suggested that NDRP might play a role in the development of neural tissues.

As strong mRNA signals were observed in olfactory epithelia, we tested the distribution of NDRP in this tissue. In olfactory epithelia of 17.5 dpc embryo, NDRP immunoreactivity was detected in the nuclei of cells aligned in approximately one-third or one-half of the thickness of epithelia from the apical surface (Fig. 2, E–F). Immunopositive molecules were mainly located at the nuclei of cells (Fig. 2E) as the locations were the same as nuclei stained by Hoechst 33258 (Fig. 2F). It is well known that developing olfactory neurons are located in an area proximal to the apical surface of olfactory epithelia (spanning approximately one-third of the width of the olfactory epithelium) in multi-rows (*18*). Since the location of NDRP immunopositive cells was similar to that of developing olfactory neurons, we suggest that NDRP-expressing cells in the olfactory epithelium are olfactory neurons. It should be noted that supporting cells were localized in a line at the most apical surface (*19*). These NDRP immunopositive cells are unlikely to be stem cells or Bowman's gland cells, because stem cells are suggested to be localized at the baseline of olfactory epithelia, and Bowman's gland cells are smaller (*20*). Interestingly, immunoreactivity in olfactory neurons was decreased after postnatal day 6, and mature olfactory neurons in adult olfactory epithelia (8-week-old mouse) had no immunoreactivity for NDRP (data not shown).

Expression Profile of NDRP in Neural Layer of Retina— In the neural layer of mouse embryonic retina, stratification is incomplete. By 17.5 dpc, an inner plexiform layer (IPL) has formed that separates the ganglion cell layer (GCL) from the neuroblastic ventricular layer (NVL) (*21*). NDRP immunoreactivity was present in both GCL and NVL (Fig. 3A). NDRP immunoreactivity in the embryonic retina is located in the nuclei of cells in GCL and both nuclei and cytoplasm of cells in NVL (Fig. 3, B and C). In contrast, the adult retina shows complete stratification into the GCL, IPL, inner granular layer (IGL), outer plexiform layer (OPL), outer granular layer (OGL), and pigment layer (PL) (*22*). We found that the expression of NDRP mRNA is high in GCL and IGL of adult retina (Fig. 3D, arrow). OGL,

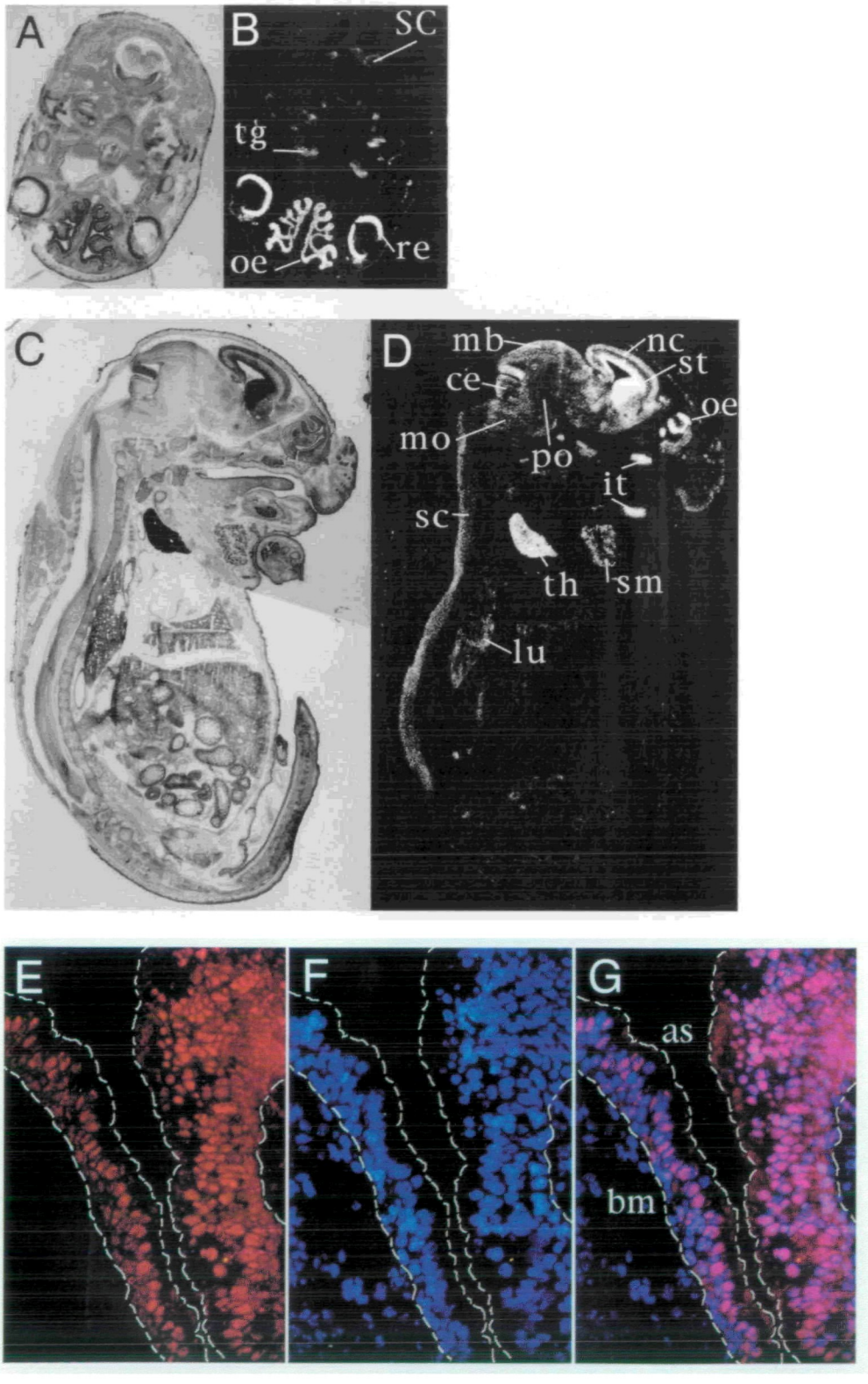

Fig. 2. **Expression of NDRP in mouse embryo.** (A–D) Nissle staining (A, C) and *in situ* hybridization of NDRP mRNA (B, D) of the head (A, B) and whole embryo (C, D) of 17.5 dpc mouse embryo are shown. Highest signals were observed in the neural layer of retina (nr) and olfactory epithelia (oe), while weak signals were seen in the trigeminal ganglia (tg) and dorsal part of the spinal cord (sc). (C, D) Sagittal section of whole 17.5 dpc embryo; strong signals were observed in olfactory epithelia (oe), striatum (st), neopallial cortex (nc), thymus gland (th), and primordium of incisor teeth (it). Moderate hybridization signals were detected in the midbrain (mb), cerebellar primordium (ce), pons (po), medulla oblongata (mo), and spinal cord (sc), while weak signals were seen in the submandibular gland (sm), and lung (lu). (E–G) Immunohistochemistry of NDRP. Location of NDRP (E), nuclei stained by Hoechst 33258 (F), and double staining of NDRP and nuclei (G) in the olfactory epithelia of 17.5 dpc mouse embryo are shown. Dashed line marked "as" indicates the apical surface of olfactory epithelia. Dashed line marked "bm" indicates the basement membrane separating reactive olfactory epithelia from connective tissue. Magnifications were 400× in (E–G). NDRP immunopositive cells were located along the apical surface and middle region of olfactory epithelia (E).

which is mainly composed of cell bodies of photoreceptor cells, showed weak NDRP mRNA expression (Fig. 3D, arrowhead). As for protein expression of NDRP in the retina, the nuclei of the neurons in both GCL and IGL were strongly labeled by anti-NDRP immunohistochemistry (Fig. 3E, arrow). Although the nuclei of the photoreceptor cells in OGL showed no immunoreactivity (Fig. 3E, asterisk), there was cytoplasmic staining in these cells (Fig. 3E, arrowhead). The presence of NDRP in both nuclei and cytoplasm in retina suggests translocation of this molecule depending on the stage of neuronal differentiation.

Expression Profile of NDRP in Dorsal Root Ganglia—We

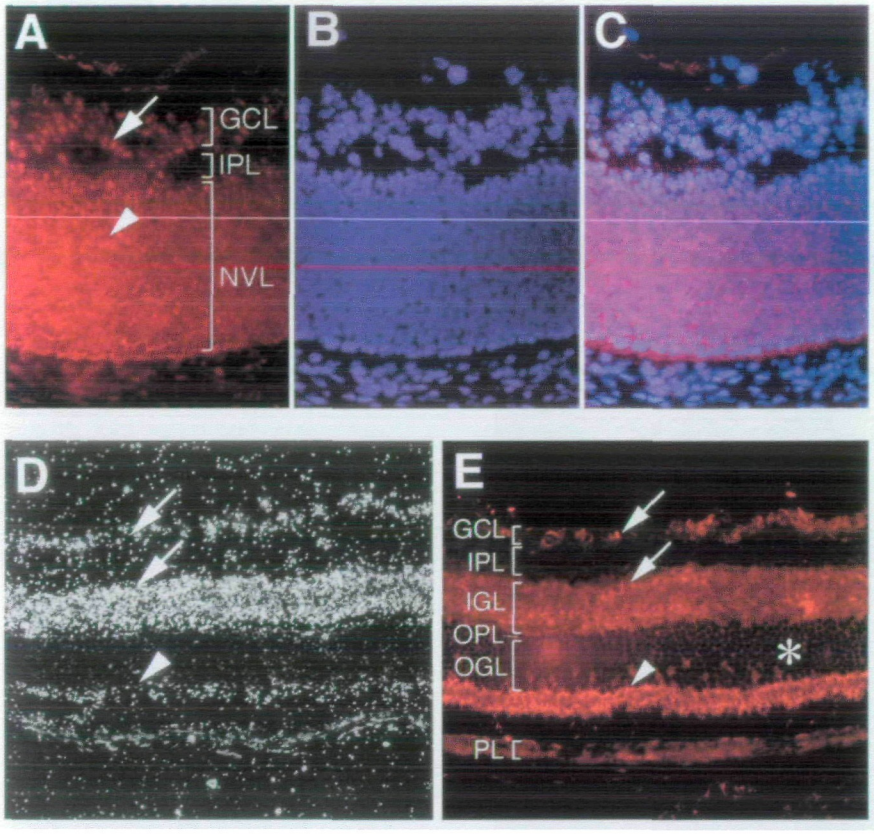

Fig. 3. **Expression of NDRP in fetal and adult retina.** (A–C) Location of NDRP (A), nuclei (B), and double staining of NDRP and nuclei (C) in the retina of 17.5 dpc mouse embryo. Arrowhead, NVL. (D) *In situ* hybridization of adult retina from 8-week-old mouse. Arrows, neurons of GCL and IGL. Arrowhead, photoreceptor cells. As faint signals over the pigment layer were not consistently observed, they were thought to be artifacts due to the irregular coating of autoradiography emulsion. (E) Immunohistochemistry of adult retina from 8-week-old mouse. Nuclei of GCL and IGL were immunopositive (arrows). Cytoplasmic regions of photoreceptor cells were also immunopositive (arrowhead). Abbreviations: GCL, ganglion cell layer; IPL, inner plexiform layer; IGL, inner granular layer; NVL, neuroblastic ventricular layer; OPL, outer plexiform layer; OGL, outer granular layer; PL, pigment layer.

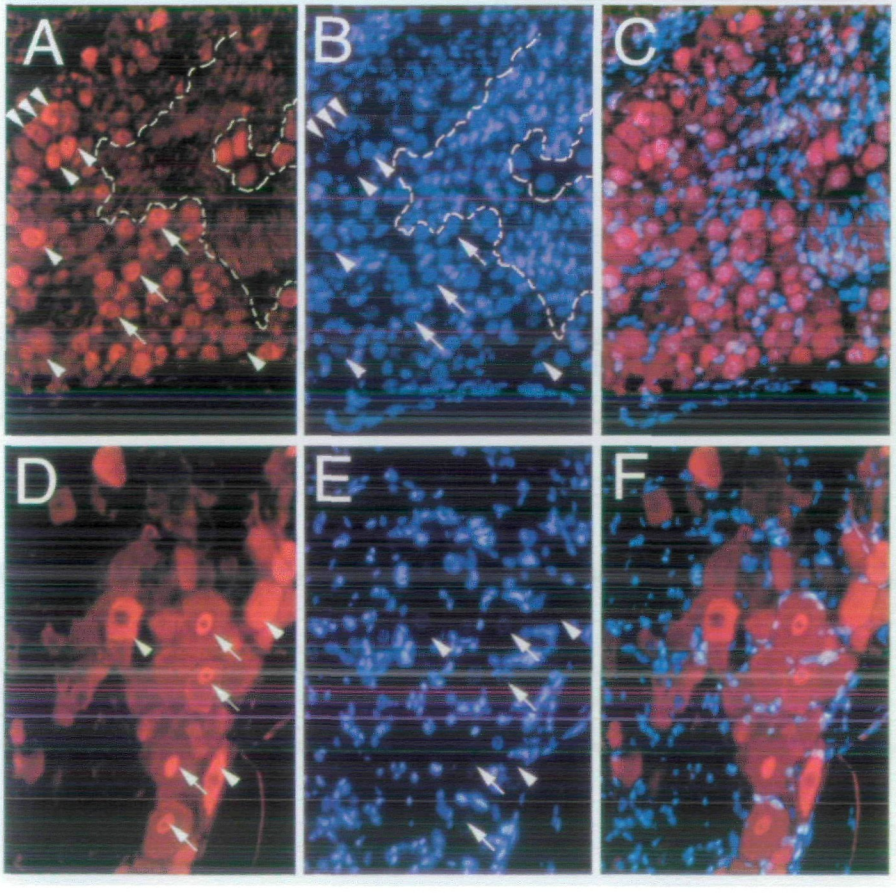

Fig. 4. **Immunohistochemical location of NDRP in DRG.** Location of NDRP (A, D), nuclei (B, E) and double staining of NDRP and nuclei (C, F) in the cervical DRG from 6-day (A–C) and 10-week (D–F) mouse are shown. (A–C) Relatively large cells were neurons in which nuclei (arrow) and cytoplasm (arrowhead) are immunopositive. Dashed line depicts the boundary between neurons and the bunch of axons. Note that small cells with oval, heterochromatic nuclei within the dashed lines (satellite cells or Schwann cells) were immunonegative for NDRP. (D–F) Adult ganglion cells are larger than those of 6-day mouse. Note that segregation of NDRP in nuclei (arrow) and cytoplasms (arrowhead) is more significant. Small cells around the ganglion neurons were satellite cells and were NDRP immunonegative.

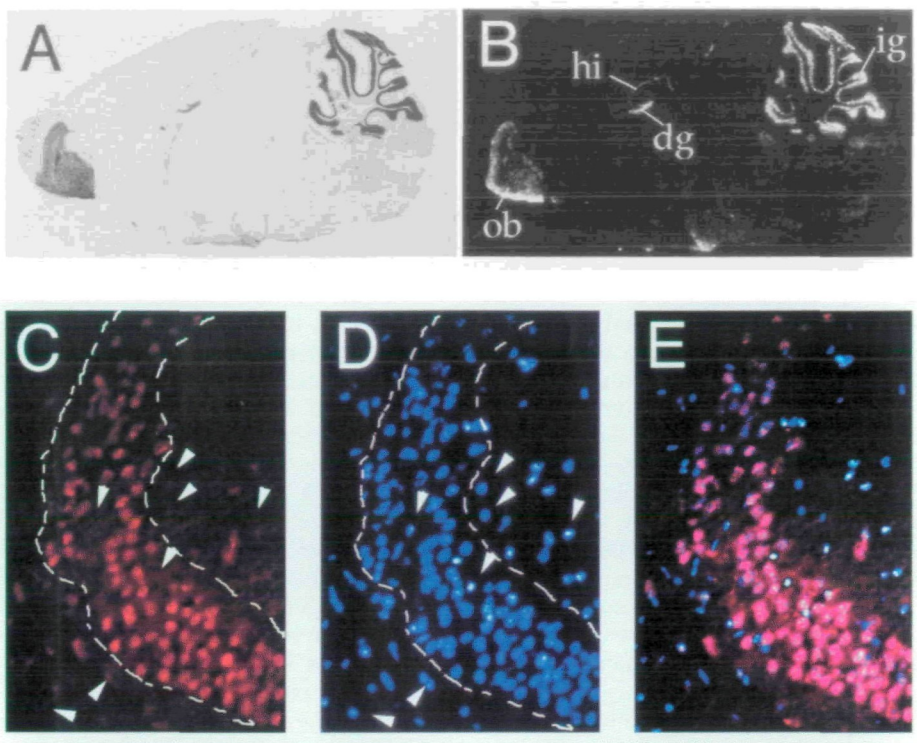

Fig. 5. **Expression of NDRP in adult brain.** (A, B) *In situ* hybridization of adult brain from 8-week–mouse. Adult brain showed the expression of message in the granular layer of the olfactory bulb (ob), hippocampus (hi), dentate gyrus (dg), and internal granular layer of the cerebellum (ig). (C–E) immunohistochemical location of NDRP in the CA3 region of hippocampus from adult mouse. Note that immunopositive cells were mainly confined to the hippocampus (inside the dashed lines) and that immunonegative cells were present inside and outside the hippocampus (arrowheads). NDRPs were located in nuclei of pyramidal cells in adult brain.

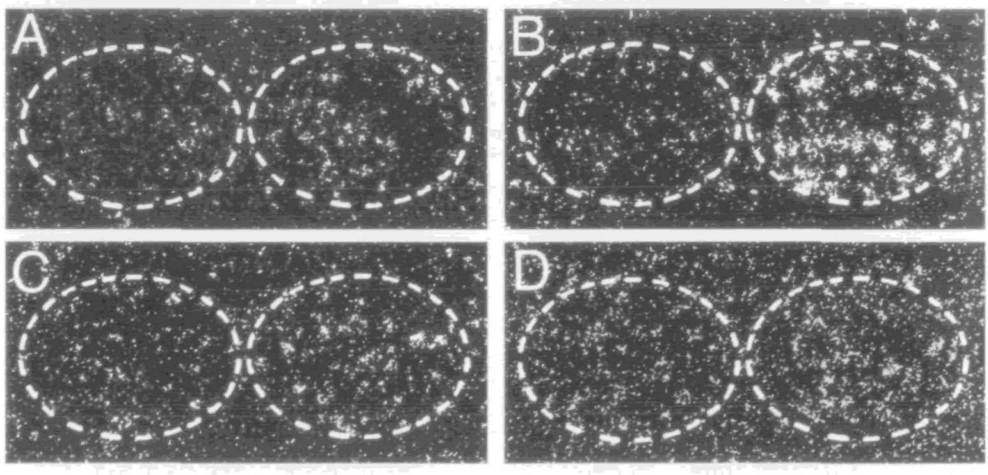

Fig. 6. **Upregulated expression of NDRP mRNA in the injured hypoglossal nerve cell bodies.** Expression of NDRP mRNA was investigated by *in situ* hybridization at 1 day (A), 3 days (B), 14 days (C), and 21 days (D) after axotomy of hypoglossal nerve of adult rat. The expression of NDRP in sham-operated nerves (left side, A–D) was under the background.

performed immunostaining of cervical dorsal root ganglion of newborn, 6-day-old and 10-week-old mouse. On day 6 after birth, DRG is mainly composed of maturing neurons in which cell proliferation has ceased (*23*). Interestingly, NDRP immunoreactivity was found in the nuclei of large cells and the cytoplasm of medium-size cells (Fig. 4, A–C). As ganglion cells in DRG are relatively large (20–40 μm) (*24*), the nuclei do not always appear in their cell bodies on thin (6 μm) sections. Therefore, these NDRP positive cells might be ganglion cells. In contrast, relatively small cells, which had oval, heterochromatic nuclei and seemed to be satellite cells and/or Schwann cells, were immunonegative (Fig. 4, A and B, inside dashed lines). The location of NDRP in adult DRG looked similar to that in 6-day-old mouse, but the segregation of the presence in nuclei and cytoplasm was more apparent. We noted that the large cells of strong nucleic staining with anti-NDRP antibody were type-A ganglion cells (Fig. 4D), which were also immunopositive for microtubule associated protein 2 (MAP2) (data not shown). These results indicate that NDRP may play a role in the differentiation or maturation of DRG neurons.

Expression Profile of NDRP in Brain—Figure 5B depicts the expression of NDRP mRNA in the brain of 8-week-old mouse. Hybridization signals were observed in the granular layer of the olfactory bulb, the pyramidal cell layer of the hippocampus, the granule cell layer of the dentate gyrus, and the granular layer of the cerebellum. As for protein expression in the hippocampus, we found strong immunoreactivity in pyramidal cells in the CA3 region (Fig. 5, C–E), while cells outside the hippocampus were mostly immunonegative (Fig. 5, C and D, outside the dashed lines). As the majority of nuclei present in the CA3 region are con-

sidered to be those of pyramidal neurons (*25*) and the anti-NDRP immunoreactivity was present in almost all of these nuclei, NDRP was likely to be expressed in the pyramidal neurons.

Increased Expression of NDRP mRNA after Motor Neuron Injury—We noted weak expression of NDRP in motor neurons in at least the spinal motor column and hypoglossal nuclei (data not shown). To explore the possible role of NDRP in the regeneration of motor neurons, we performed *in situ* hybridization of NDRP transcripts on the hypoglossal nuclei after axotomy of hypoglossal nerve. As shown in Fig. 6, NDRP mRNA signals increased in the hypoglossal nuclei on the operated side, but not on the sham-operated side, 3 days (Fig. 6B) to 14 days (Fig. 6C) after axotomy. The level of mRNA expression returned to the control level 21 days after axotomy (Fig. 6D). These results suggested that the mRNA of NDRP in functional motor neurons was very low, whereas the expression of NDRP was increased in the regenerating cells, as is in the case for other neuron-associated genes (*26*). We could not, however, rule out the possibility of NDRP expression in microglia and astrocytes.

Although NDRP cDNA was isolated from Wobbler mouse, and the mRNA was expected to be upregulated in this disease model animal, the expression of NDRP was not significantly different from that in control mouse (data not shown).

DISCUSSION

NDRP contains six WD repeats. The family of WD repeat proteins is characterized by the presence of series of four to eight conserved repeating units of amino acids, usually beginning with GH and ending with WD (core region), separated by short, variable sequences (non-core regions) (*12*, *13*). These non-core regions are thought to be exposed on the surface of the molecule and to be involved in the specificity of interaction with other proteins (*12*). From this point of view, NDRP may have a unique function, since the amino acid sequences of the variable regions in NDRP have no similarity with those in any so far known WD repeat proteins. NDRP has multiple NLSs in the C-terminal half of the sequence and is here demonstrated to be localized in most cases in the nuclei of neuronal cells, depending on the stage of neural differentiation. The amino acid sequence of NDRP exhibited the absence of any type of motif of transcription factors. Proteins which contain WD repeats are generally regulatory proteins, and none has been shown to have an enzymatic activity (*12*). Thus, it is likely that the NDRP might regulate protein–protein interaction and/or the function of other molecules like transcription factors or nuclear proteins. Taken together with our finding that NDRP is expressed in developing neurons and, in particular, in regenerating motor neurons, it is interesting to note that Groucho-like transcription factor UNC-37, a WD repeat–containing protein, is known to specify motor neuron identity and synaptic choice in *Caenorhabditis elegans* (*4*).

We have found that NDRP shows the highest expression in olfactory epithelia, the neural layer of retina and DRG. During late embryonic development, olfactory neurons develop dramatically and complete the differentiation mostly before birth (*27*, *28*). During development, stem cells called olfactory placode in epithelia migrate from the basal layer towards the surface, concomitantly sprouting apical and basal processes. At this time, immature olfactory neurons are typical bipolar-shaped cells. The apical processes eventually reach the epithelial surface and differentiate into ciliated dendrites, whereas the basal processes pass through basal layer of epithelia and finally project axons into the olfactory bulb. NDRP immunoreactivity was detected in the nuclei of cells aligned along the apical surface and occupying one-third to one-half of the thickness of olfactory epithelia (Fig. 5, A and B). Olfactory marker protein (OMP) is known to be expressed in developing olfactory neurons (*29*), and OMP-positive neurons are located in an area proximal to the apical surface of olfactory epithelia (spanning approximately one third of the width of the olfactory epithelium) in multi-rows (*18*). The location of NDRP positive cells is similar to that of OMP-positive cells, and just over the immature olfactory neurons, which are type III beta tubulin–immunoreactive (*30*, *31*). Furthermore, we noted by using anti–rat OMP antibody, that most OMP-positive cells in olfactory epithelia from rat embryo were also immunopositive for NDRP (data not shown). From these results, we considered that NDRP-immunopositive cells were developing olfactory neurons. By using antibodies to microtubule-associated protein 2 (MAP2) and glial fibrillary acidic protein (GFAP), we have examined their expression in NDRP-positive cells. The results were both negative (data not shown), which were consistent with the previous observation that olfactory neurons were immunoreactive to neither MAP2 (*32*) nor GFAP antibody. MAP2 and GFAP immunopositive cells were located at more basal regions of olfactory epithelia, namely, around the stem cells. Interestingly, NDRP immunoreactivity in olfactory epithelia was decreased after birth, and mature olfactory neurons in adult olfactory epithelia had no NDRP immunoreactivity (data not shown). Thus, it is interesting to speculate that NDRP positive cells might be developing olfactory neurons, which are migrating to the epithelial surface and sprouting the ciliated dendrites and axons.

In contrast to the olfactory neuronal systems, the neuronal network and stratification of retina are known to be completed after birth (*33*, *34*). We showed that NDRP was expressed in both the ganglion cell layer (GCL) and the neuroblastic ventricular layer (NVL) during embryonic development. In these layers, NDRP was located in the nuclei of cells in GCL or in both the nuclei and cytoplasm in cells in NVL. In adult retina, when stratification of the neural layer was completed, strong mRNA hybridization signals and immunoreactivity were observed in GCL and the internal granular layer (IGL). GCL is mainly composed of ganglion cells whose dendrites and axons are well polarized, whereas IGL is composed of bipolar cells, amacrine cells and horizontal cells. NDRP in these matured neurons was located exclusively in the nuclei, indicating that the NDRP had been translocated to the nuclei during neural differentiation.

We have analyzed DRG from 6-day-old newborn mice and 10-week-old adult mouse, as the DRG neurons on day 6 have ceased cell division and are large enough to be judged as neurons morphologically (*24*). During embryonic development, the immature neurons are bipolar, and they undergo a remarkable morphological change, termed pseudo-unipolarization, to their mature form (*35*). On postnatal day 6, DRG is devoid of normal dendrites, but instead

has a single trunk that divides into central and peripheral processes at some distance from the cell body. As the development of mouse body is dramatic in the first few days after birth, increase in cell size, myelination, and elongation of axons of DRG neurons may be remarkable during this period. NDRPs are located in both nuclei and cytoplasm in DRG neurons when examined on day 6. In mature DRG neurons in adult mice, we noted that large cells which had significant NDRP immunostaining in the nuclei were large, light, type-A ganglion cells (data not shown) which had abundant MAP2 immunostaining (*36*). In addition, ganglion cells with strong NDRP immunoreactivity in only the cytoplasm showed no MAP2 expression. Thus, it is tempting to speculate that a certain external and/or intrinsic signal may regulate the translocation and function of NDRP in the differentiating DRG neurons. In this connection, it may be worth noting that well-polarized mature neurons in retina, olfactory epithelia and brain are immunopositive for NDRP in the nuclei.

In adult brain, NDRP immunoreactivity was found in the nuclei of granule cells in the olfactory bulb, pyramidal cells of the hippocampus, granule cells of the dentate gyrus, and granular cells of the cerebellum. Granule cells of the olfactory bulb and cerebellum are interneurons with 3 to 5 dendrites and short axons. Pyramidal cells of the hippocampus are well-polarized neurons with bidirectional dendrites projecting into stratum oriens and stratum radiatum and long efferent axons. Granule cells of dentate gyrus are interneurons with rich dendrites and relatively short axons, making connections from afferent axons to pyramidal cells of hippocampal CA3 and CA4 regions. The function of NDRP in these well-polarized mature neurons remains to be determined. However, it should be noted that rearrangement and new formation of synapses are highly expected in these regions with NDRP-positive cells (*37–39*), suggesting a role of NDRP in these events.

We demonstrated upregulated expression of NDRP in the hypoglossal nerve after axotomy. Injured motor neurons are known to revert to an immature phenotype and then regenerate to mature neurons during the period of reinnervation, normally between 2 and 4 weeks after axotomy (*26*). Thus, it is tempting to speculate that the expression of NDRP mRNA is induced upon injury of motor neurons, at early stages of regeneration, presumably to promote the elongation of axons. In this respect, it might be reasonable that the expression of NDRP mRNA should be reduced to control level after the recovery of neuromuscular junctions.

In summary, the present study showed the identification of a novel gene, NDRP. Although the precise function of NDRP remains to be tested, the strong expression of NDRP in developing and regenerating neurons suggest its importance in neuronal differentiation.

We thank Dr. F.L. Margolis, for anti-rat OMP antibody. We also thank Y. Nakamura for secretarial assistance, and R. Watebe for technical help. This work was supported by Grant-in-Aid from the Ministry of Education, Science, Sports and Culture, Human Frontier Science Program, Ichiro Kanehara Foundation, Inamori Foundation, Kato Memorial Bioscience Foundation, and Naito Foundation.

REFERENCES

1. Garcia-Higuera, I., Fenoglio, J., Li, Y., Lewis, C., Panchenko, M.P., Reiner, O., Smith, T.F., and Neer, E.J. (1996) Folding of proteins with WD-repeats: comparison of six members of the WD-repeat superfamily to the G protein beta subunit. *Biochemistry* **35**, 13985–13994
2. Jansen, R., Tollervey, D., and Hurt, E.C. (1993) A U3 snoRNP protein with homology to splicing factor PRP4 and G beta domains is required for ribosomal RNA processing. *EMBO J.* **12**, 2549–2558
3. Chen, G., Nguyen, P.H., and Courey, A.J. (1998) A role for Groucho tetramerization in transcriptional repression. *Mol. Cell. Biol.* **18**, 7259–7268
4. Pflugrad, A., Meir, J.Y.-J., Barnes, T.M., and Miller, D.M., III (1997) The Groucho-like transcription factor UNC-37 functions with the neural specificity gene unc-4 to govern motor neuron identity in *C. elegans*. *Development* **124**, 1699–1709
5. Saxena, K., Gaitatzes, C., Walsh, M.T., Eck, M., Neer, E.J., and Smith, T.F. (1996) Analysis of the physical properties and molecular modeling of Sec 13: a WD repeat protein involved in vesicular traffic. *Biochemistry* **35**, 15215–15221
6. Mishima, M. and Nishida, E. (1999) Coronin localizes to leading edges and is involved in cell spreading and lamellipodium extension in vertebrate cells. *J. Cell Sci.* **112**, 2833–2842
7. Humphery, T. and Enoch, T. (1998) Sum1, a highly conserved WD-repeat protein, suppresses S-M checkpoint mutants and inhibits the osmotic stress cell cycle response in fission yeast. *Genetics* **148**, 1731–1742
8. Mitsumoto, H., Ikeda, K., Kinkosz, B., Cedarbaum, J.M., Wong, V., and Lindsay, R.M. (1994) Arrest of motor neuron disease in *wobbler* mice cotreated with CNTF and BDNF. *Science* **265**, 1107–1110
9. Ikeda, K., Kinoshita, M., Tagaya, N., Shiojima, T., Taga, T., Yasukawa, K., Suzuki, H., and Okano, A. (1996) Coadministration of interleukin-6 (IL-6) and soluble IL-6 receptor delays progression of wobbler mouse motor neuron disease. *Brain Res.* **726**, 91–97
10. Kiryu, S., Yao, G.L., Morita, N., Kato, H., and Kiyama, H. (1995) Nerve injury enhances rat neuronal glutamate transporter expression: Identification by differential display PCR. *J. Neurosci.* **15**, 7872–7878
11. Hornung, R.L., Longo, D.L., Gowda, V.L., and Kwak, L.W. (1995) Induction of $CD8^+$ cytotoxic lymphocyte response to a soluble antigen given together with a novel muramyl dipeptide adjuvant, *N*-acetyl-D-glucosaminyl-(β1-4)-*N*-acetylmuramyl-L-alanyl-D-isoglutamine (GMDP). *Ther. Immunol.* **2**, 7–14
12. Neer, E.J., Schmidt, C.J., Nambudripad, R., and Smith, T.F. (1994) The ancient regulatory-protein family of WD-repeat proteins. *Nature* **371**, 297–300
13. Smith, T.F., Gaitatzes, C., Saxena, K., and Neer, E.J. (1999) The WD repeats: a common architecture for diverse functions. *Trends Biochem. Sci.* **24**, 181–185
14. Hicks, G.R. and Raikhel, N.V. (1995) Protein import into the nucleus: an integrated view. *Annu. Rev. Cell. Div. Biol.* **11**, 155–188
15. Robbins, J., Dilworth, S.M., Laskey, R.A., and Dingwall, C. (1991) Two interdependent basic domains in nucleoplasmin nuclear targeting sequence: identification of a class of bipartite nuclear targeting sequence. *Cell* **64**, 615–623
16. Imai, H., Osumi-Yamashita, N., Ninomiya, Y., and Eto, K. (1996) Contribution of early-migrating midbrain crest cells to the dental mesenchyme of mandibular molar teeth in rat embryo. *Dev. Biol.* **176**, 151–165
17. Luukko, K. (1998) Neuronal cells and neurotrohins in odontogenesis. *Eur. J. Oral Sci.* **106**, 80–93
18. Farbman, A. and Margolis, F. (1980) Olfactory marker protein during ontogeny: Immunohistochemical localization. *Dev. Biol.* **74**, 205–215
19. Costanzo, R.M. and Gradiadei, P.P.C. (1983) A quantitative analysis of changes in the olfactory epithelium following bulbectomy in hamster. *J. Comp. Neurol.* **215**, 370–381
20. Schwob, J.E., Farber, N.B., and Gottlieb, D.I. (1986) Neurons of olfactory epithelium in adult rats contain vimentin. *J. Neurosci.* **6**, 208–217

21. Hinds, J.W. and Hinds, P.L. (1983) Development of retinal amacrine cells in the mouse embryo: Evidence for two models of formation. *J. Comp. Neurol.* **213**, 1–23
22. Maslim, J. and Stone, J. (1988) Time course of stratification of the dendritic fields of ganglion cells in the retina of the cat. *Brain Res. Dev. Brain Res.* **44**, 87–93
23. Lawson, S.N., Caddy, K.W.T., and Biscoe, T.J. (1974) Development of rat dorsal ganglion neurons: Studies of cell birthday and change in mean cell diameter. *Cell. Tiss. Res.* **153**, 399–413
24. Larnicol, N., Rose, D., and Duron, B. (1991) Postnatal development of small and large dorsal root ganglion neurons in the cat. A study on cervical levels (C5-C6) and on phrenic afferents. *Neurosci. Lett.* **121**, 93–96
25. Wedzony, K. and Czyrak, A. (1997) The distribution of the NMDA R1 subunit in the rat hippocampus—an immunocytohistochemical study. *Brain Res.* **768**, 333–337
26. Chiu, A.R., Chen, E.D., and Loera, S. (1993) A motor neuron-specific epitope and the low-affinity nerve growth factor receptor display reciprocal patterns of expression during development, axotomy, and regeneration. *J. Comp. Neurol.* **328**, 351–363
27. Cuschieri, A. and Bannister, L.H. (1975) The development of the olfactory mucosa in the mouse: light microscopy. *J. Anat.* **119**, 277–286
28. Klein, S.L. and Gradziadei, P.P.C. (1983) The differentiation of the olfactory placode in *Xenopus laevis*: A light and electron microscope study. *J. Comp. Neurol.* **217**, 17–30
29. Mirafall, F. and Monti Graziadei, G.A. (1982) Experimental studies on the olfactory marker protein. II. Appearance of the olfactory marker protein during differentiation of the olfactory sensory neurons of mouse: an immunohistochemical and autoradiographic study. *Brain Res.* **239**, 245–250
30. Lee, V.M. and Pixley, S.K. (1994) Age and differentiation-related differences in neuron-specific tubulin immunostaining of olfactory sensory neurons. *Dev. Brain Res.* **83**, 209–215
31. Roskams, A.J.I., Cai, X., and Ronnet, G.V. (1998) Expression of neuron-specific beta-III tubulin during olfactory neurogenesis in the embryonic and adult rat. *Neuroscience* **83**, 191–200
32. Kaakkloa, S., Palo, J., Malmberg, H., Sulkava, R., and Virtanen, I. (1994) Neurofilament profile in olfactory mucosa of patients with a clinical diagnosis of Alzheimer's disease. *Virchows Arch.* **424**, 315–319
33. Maslin, J. and Stone, J. (1986) Synaptogenesis in the retina of the cat. *Brain Res.* **373**, 35–48
34. Niiya, A., Ohto, H., Kawakami, K., and Araki, M. (1998) Localization of Six4/AREC3 in the developing mouse retina; implication in mammalian retinal development. *Exp. Eye Res.* **67**, 699–707
35. Matsuda, S., Baluk, P., Shimizu, D., and Fujiwara, T. (1996) Dorsal root ganglion neuron development in chick and rat. *Anat. Embryol.* **193**, 475–480
36. Hall, A.K., Ai, X., Hickman, G.E., MacPhedran, S.E., Nduaguba, C.O., and Robertson, C.P. (1997) The generation of neural heterogeneity in a rat sensory ganglion. *J. Neurosci.* **17**, 2775–2784
37. Kaba, H., Rosser, A., and Keverne, B. (1989) Neural basis of olfactory memory in the context of pregnancy block. *Neuroscience* **32**, 657–662
38. Bloedel, J.R. (1987) The cerebellum and memory storage. *Science* **238**, 1728–1729
39. Tsukahara, N. and Oda, Y. (1981) Appearance of new synaptic potentials at corticorubral synapses after the establishment of classical conditioning. *Proc. Jpn. Acad.* **57B**, 398–401